DISTRIBUTION STATEMENT A. Approved for public release; distribution is unlimited.

Classical and Non-Classical Regimes of the Limited-Fetch Wave Growth and Localized Structures on the Surface of Water

Vladimir Zakharov, Andrei Pushkarev
Waves and Solitons LLC
1719 W. Marlette Ave.
Phoenix, AZ 85015
phone: +1 (602) 748-4286 e-mail: dr.push@gmail.com

Award Number: N00014-10-1-0991

LONG TERM GOALS:

Development of accurate and fast advanced statistical and dynamical nonlinear models of ocean surface waves, based on first physical principles, which will improve and accelerate both long term ocean surface waves forecasts and prediction of strongly coherent events, such as freak waves, tsunami and wave-breakings.

OBJECTIVES:

Study of non-stationary limited fetch waves growth in presence of wind; interpretation of altimeter data through study of self-similar solutions of Hasselmann equation; studying of integrability of 1D Zakharov equation for surface waves; study of the possibility of generalization of compact 1D water waves equation for 2D situation; study of the implications of modulational instability on solitons, rogue waves and air-surface interaction; study of 1D approximate model of deep water surface waves

APPROACH

Numerical methods for solution of integro-differential equations; analytical self-similar solutions for integro-differential equations; Hamiltonian formalism; comparison of analytical and numerical solutions with experimental data; analytical and numerical solution of approximate model for deep water surface waves

WORK COMPLETED:

- Non-stationary fetch limited numerical simulation: classical and non-classical regimes.
- Physical model of sea wave period from altimeter data
- Prove of non-integrability of 1-D Zakharov equation and generalization of compact equation for almost 1-D waves
- Study of modulational instability and its implications for solitons, rogue waves and air-surface interactions
- Approximate model for 1D deep water surface waves based on MMT equation

RESULTS

1. Non-stationary fetch limited numerical simulation. Classical and non-classical regimes.

During reported year we continued to study Hasselmann equation for energy spectral density $\varepsilon(\vec{r},\vec{k},t)$

$$\frac{\partial \varepsilon}{\partial t} + \frac{\partial \omega_k}{\partial \vec{k}} \frac{\partial \varepsilon}{\partial \vec{r}} = S_{nl} + S_{wind} + S_{diss} \tag{1}$$

for the simplified, but real physical situation, which includes the most important component of the general statement -- non-stationarity in time, exact nonlinearity S_{nl}, wind forcing term S_{wind} and wave dissipation term S_{diss} due to wave-breaking.

Such simplified formulation is the limited fetch wind growth situation, where Hasselmann equation is reduced to

$$\frac{g}{2\omega} \cos\theta \frac{\partial \varepsilon}{\partial x} = S_{nl} + S_{wind} + S_{diss} \tag{2}$$

where $\boldsymbol{x}$ is the spatial coordinate, orthogonal to the shore, and θ is the angle between individual wavenumber $\boldsymbol{k}$ and the axis $\boldsymbol{x}$.

This situation is presented schematically on the following diagram:

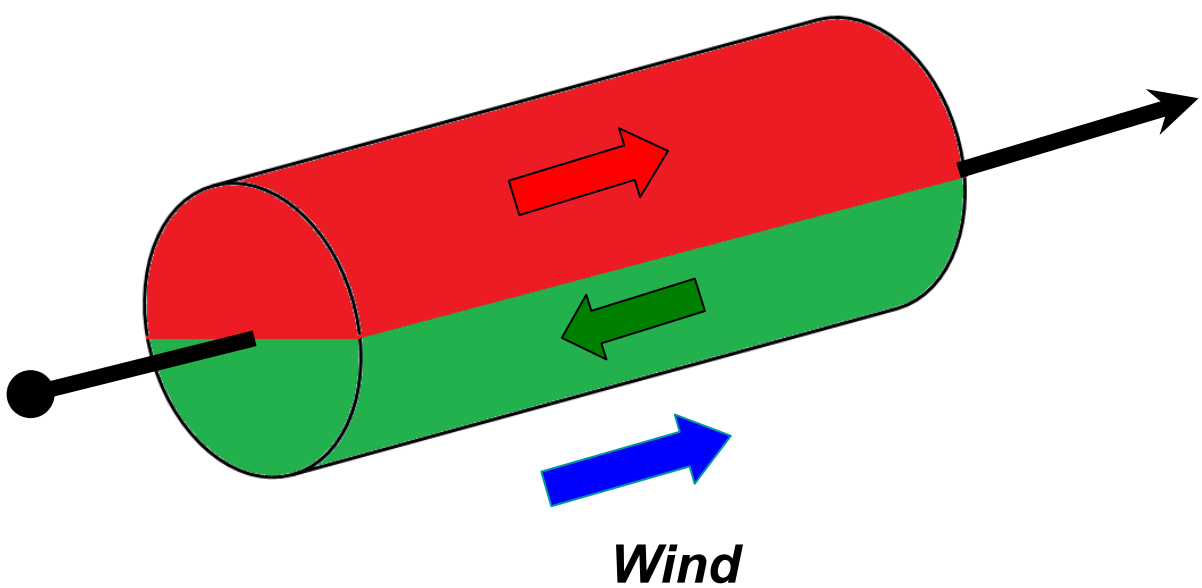

Fig.1 Schematic description of the energy fluxes along the fetch in real and Fourier spaces.

Black axis represents the real space axis ***x*** ortogonal to the shore line, red/green cylinder show Fourier-space of the system. Red part of the cylinder corresponds to positive advection velocity in front of time derivative of Hasselmann ***Eq.(2)*** (red arrow is directed away from the shore), while green part of the cylinder corresponds to negative advection velocity (green arrow directed toward the shore), in correspondence with the $\cos\theta$ in ***Eq.(2)***. Such schematic picture suggests that limited fetch growth consists of essentially three different processes happening in real and Fourier spaces: (i) energy advection away the shore in real space (red tube); (ii) energy advection toward the shore in real space (green tube); (iii) nonlinear interaction of the waves between red and green parts of the tube in Fourier space for any given point of the fetch and time.

For the solution of ***Eq.(2)*** we need to know the source terms in its right-hand side. The procedure of exact calculation of S_{nl} term is well-known and given by Webb-Resio-Tracy algorithm. The parameterization of the wind input term S_{in} is given by (see **[R1]**) :

$$S_{wind} = 0.159\frac{\rho_{air}}{\rho_{water}}\omega\left(\frac{\omega}{\omega_0}\right)^{4/3} f(\theta), \quad f(\theta) = \begin{cases} \cos\theta \text{ for } -\pi/2 \le \theta \le \pi/2 \\ 0 \text{ otherwise} \end{cases} \tag{3}$$

$$\omega_0 = \frac{g}{u_{10}}, \quad \frac{\rho_{air}}{\rho_{water}} = 1.3\cdot 10^{-3}$$

and is based on the fact that ***Eq.(2)*** has self-similar solution

$$\varepsilon = x^{p+q}F(\omega x^q) \tag{4}$$

with parameters

$$q = \frac{3}{10}, \quad p = 1, \; s = \frac{4}{3} \tag{5}$$

along with the fact of fitting the experimental data by specific regression line, see **[R2], [R3].**

The contribution of the dissipation term S_{diss} was calculated similar to **[R3],** where white-capping dissipation term was introduced implicitly through f^{-5} ($f = \frac{\omega}{2\pi}$) energy spectral tail stretching in frequency range from $f_d = 1.1$ to $f_{\max} = 2.0$.

We solved Cauchy problem for the ***Eq.(2)*** for the following set parameters

- Fetch size 40 km
- Number of nodes 40
- 72 logarithmic frequencies
- 36 points angle resolution
- Wind speed $U_{10} = 5m/\sec$

which translates into:

• Characteristic angular frequency $\omega_{cr} = g / U_{10} = 2 rad / \sec$

• Characteristic linear frequency $f_0 = 1.1 Hz$

• Dimensionless fetch $\chi = \frac{L}{U_{10}^2} g = 1.6 \cdot 10^4$

Initial conditions were chosen in the form of low-amplitude noise in the red part of the Fourier space and zero in the green part of the phase space cylinder (see ***Fig. 1***).

Fig.2 represents total energy of the fetch as a function of time. One can see that energy growth evolution can be split into two parts -- first of relatively fast growth for time less than 4 hr, and the second part of relatively slow growth.

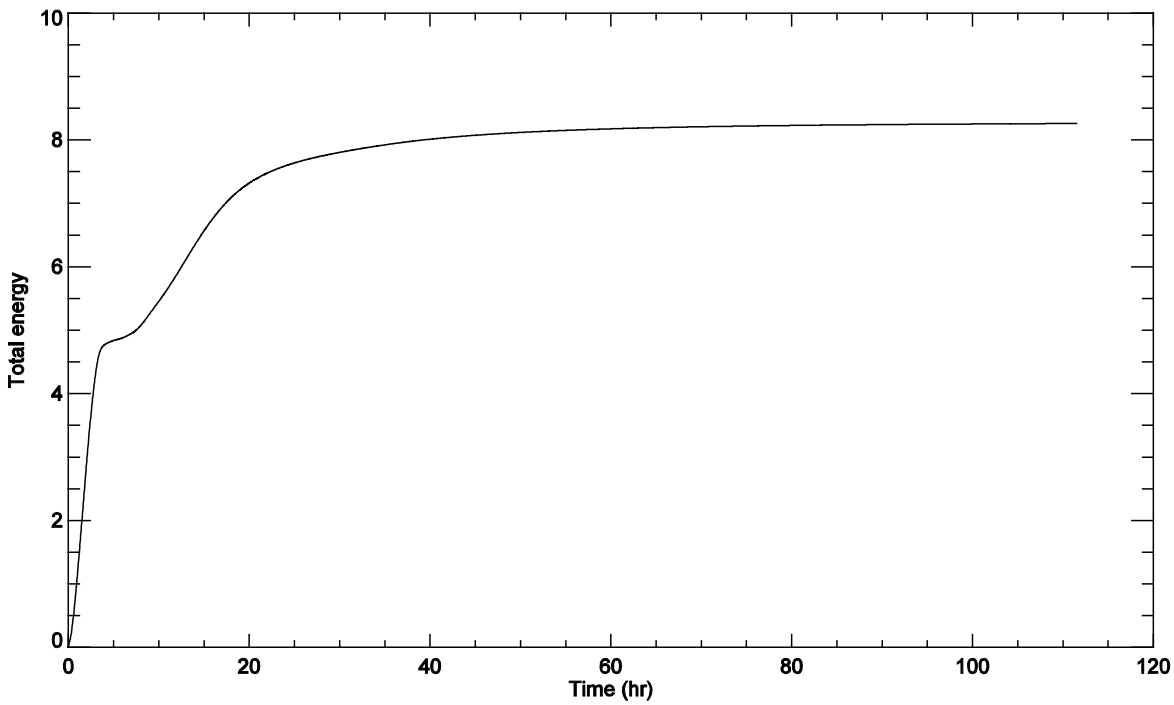

Fig.2 Total energy of the fetch as a function of time.

Comparison of the phase space distributions of the spectrum for ***t=2hr*** (see ***Fig.5 a,b***), ***t=8hr*** (see ***Fig.6 a,b***) and ***t=24hr*** (see ***Fig.7 a,b***) shows qualitative difference in their shape, too.

For earlier times ***t=2hr*** the shape of the spectrum has the shape of the single hump, growing with the distance from the shore along the fetch. For later times ***t=8hr*** and ***t=24hr*** the shape of the spectrum is more complex: besides classical center single-hump of the energy spectrum, growing away from the shore, one can see side satellites in the form of spikes, corresponding to waves propagating along the shore.

Furthermore, the direction of those waves propagating along the shore is getting slanted toward the shore with the distance diminishing toward the shore. Closer to the shore, the waves are propagating at 15 degrees toward the shore line. This observation is quite remarkable: it means that long enough

excitation of the waves in time by the wind blowing away from the shoreline, finally excites the waves coming against the wind toward the shore.

Fig.3 represents distribution of energy along the fetch for different times. One can see that energy behavior for time less than ***4 hr*** is described by threshold-like behavior propagating along the fetch, in correspondence with **[R4].**

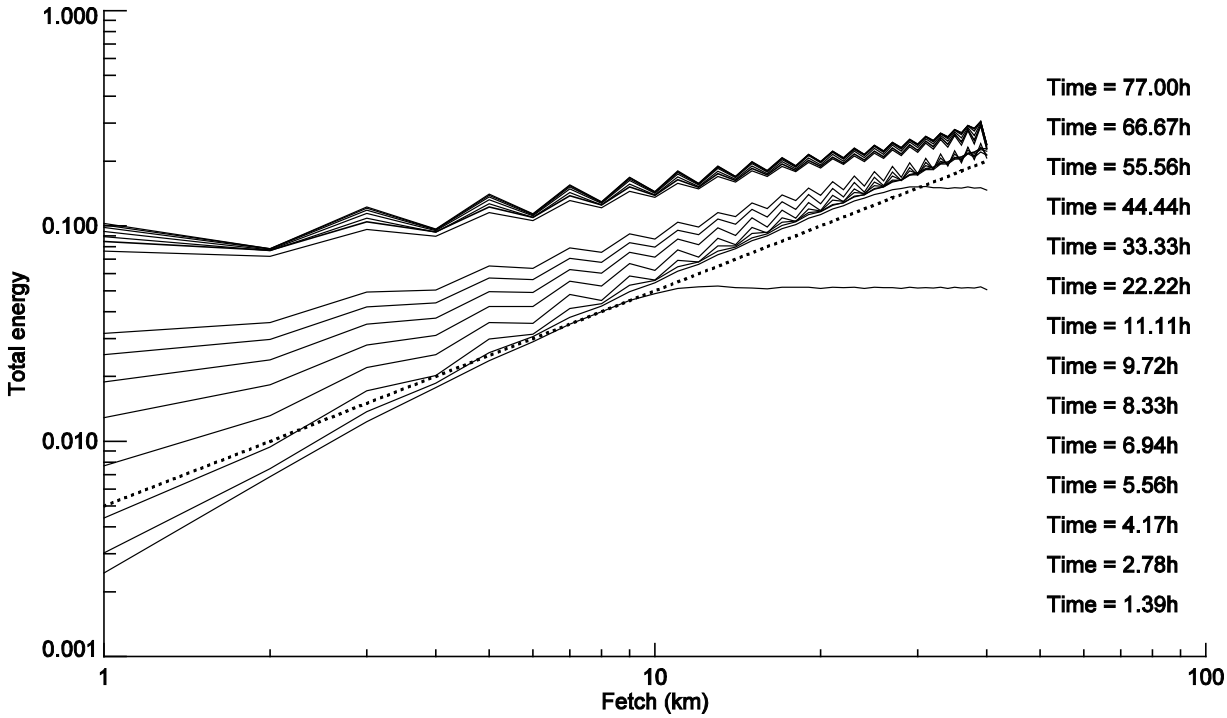

Fig.3 Energy distribution along the fetch. Dotted line -- linear function.

At time around ***4 hr***, the energy growth is approximated by linear function of the fetch distance. This dependence was predicted in **[R5]** through self-similarity analysis: it was shown that for fetch-limited self-similar solution the dimensionless energy $\widetilde{E} = \dfrac{E \cdot g^2}{U^4} = a\chi$. For time ***t = 4 hr***, we get from numerical simulation results $a = 2.4 \cdot 10^{-7}$. ***Table 1*** represents experimental data (see **[R5]**) on measuring the constant $\boldsymbol{a}$ for different experiments. One can see good correspondence of our numerical simulation and experimental predictions:

Table 1. Results of measurements of the constant a for four different experimental observations.

Experiment	a
Nakata Bay (Mitsuyasu et al., 1971)	2.89×10^{-7}
JONSWAP (Hasselmann et al., 1973)	1.6×10^{-7}
Lake St. Clair (Donelan et al., 1992)	1.7×10^{-7}
Bothnian Sea (Kahma, 1981)	2.6×10^{-7}

Fig.4 shows mean frequency distribution along the fetch for different moment of time less than ***4 hr***. One can see that the portion of the "threshold-like" function is closely described by self-similar solution ***Eqs.(4)-(5)*** :

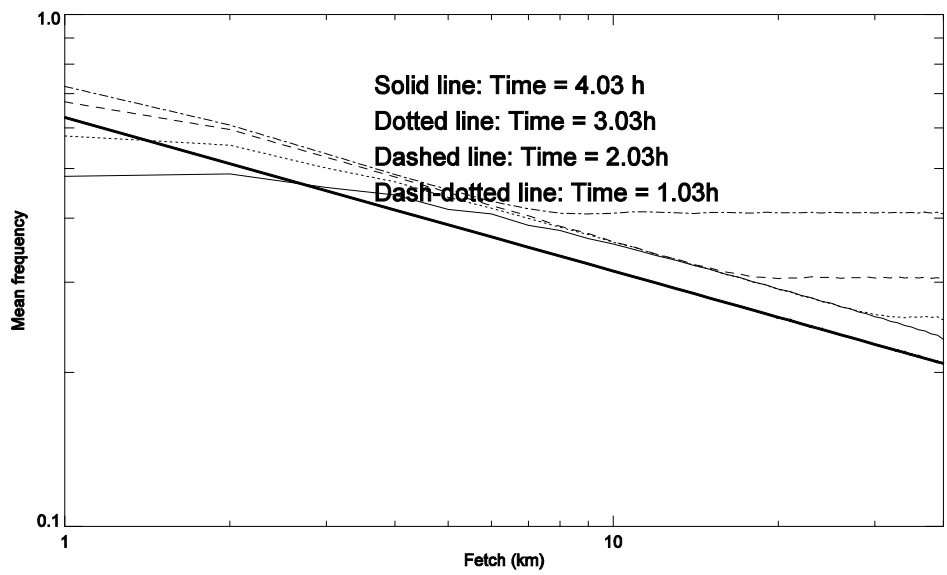

Fig.4 Logarithm of mean frequency distribution as a function of the logarithm of fetch for four different moments of time: 1 hr, 2 hr, 3 hr and 4 hr. Solid line -- self-similar prediction q=0.3 from Eqs.(4)-(5)

All the above facts clearly show that limited fetch growth in the channels of final width can be split in time for two different physical regimes.

The first regime corresponds to self-similar solution developing for the characteristic times defined by ratio of the channel width to characteristic advection velocity of the wave field and could be called classical. This regime corresponds mainly to energy advection in the red part of the cylinder on ***Fig.1***.

The second regime is happening later in time when the energy starts to reflect from the opposite boundary condition and corresponds to energy advection against the wind in the green cylinder on ***Fig.1***. It exhibits itself in waves generating predominantly parallel to the shore line, tending to slant toward the shore, as approaching to the beginning of the fetch, at 15 degrees.

To wrap the results of research up, our numerical experiments show existence of 2 regimes of wave turbulence in the limited fetch conditions:

- classical regime as a combination of self-similar regimes for moderate duration $\tau < 3 \cdot 10^4$
- non-classical regime exhibiting in waves propagating almost parallel to the coastal line (about 15 degrees near the shore) analogous to Bose-condensation for $\tau > 3 \cdot 10^4$

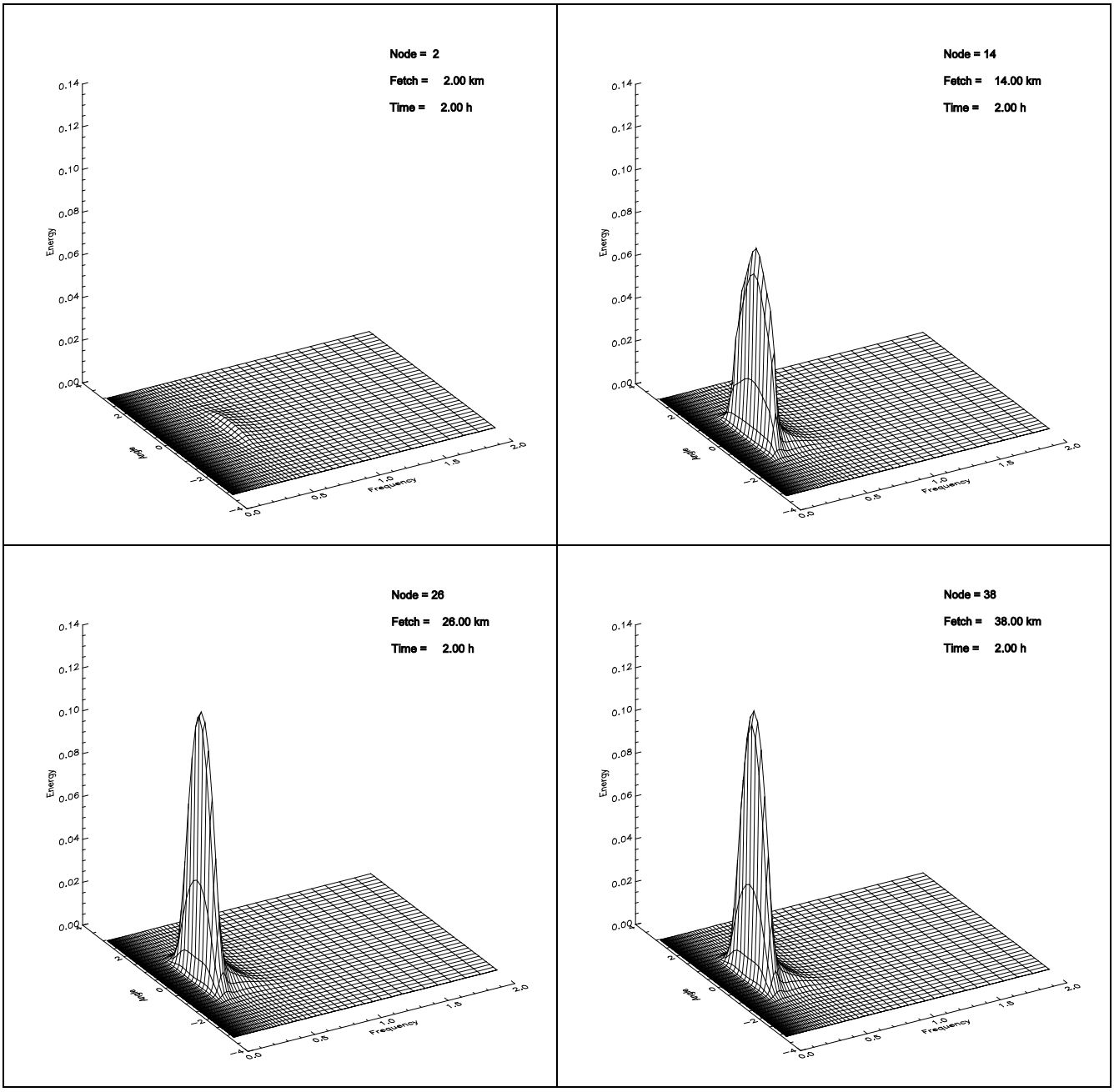

Fig.5a Spectral energy distribution as a function of frequency f and angle θ at the fetch distances 2 km, 14 km, 26 km, 38 km for time 2hr.

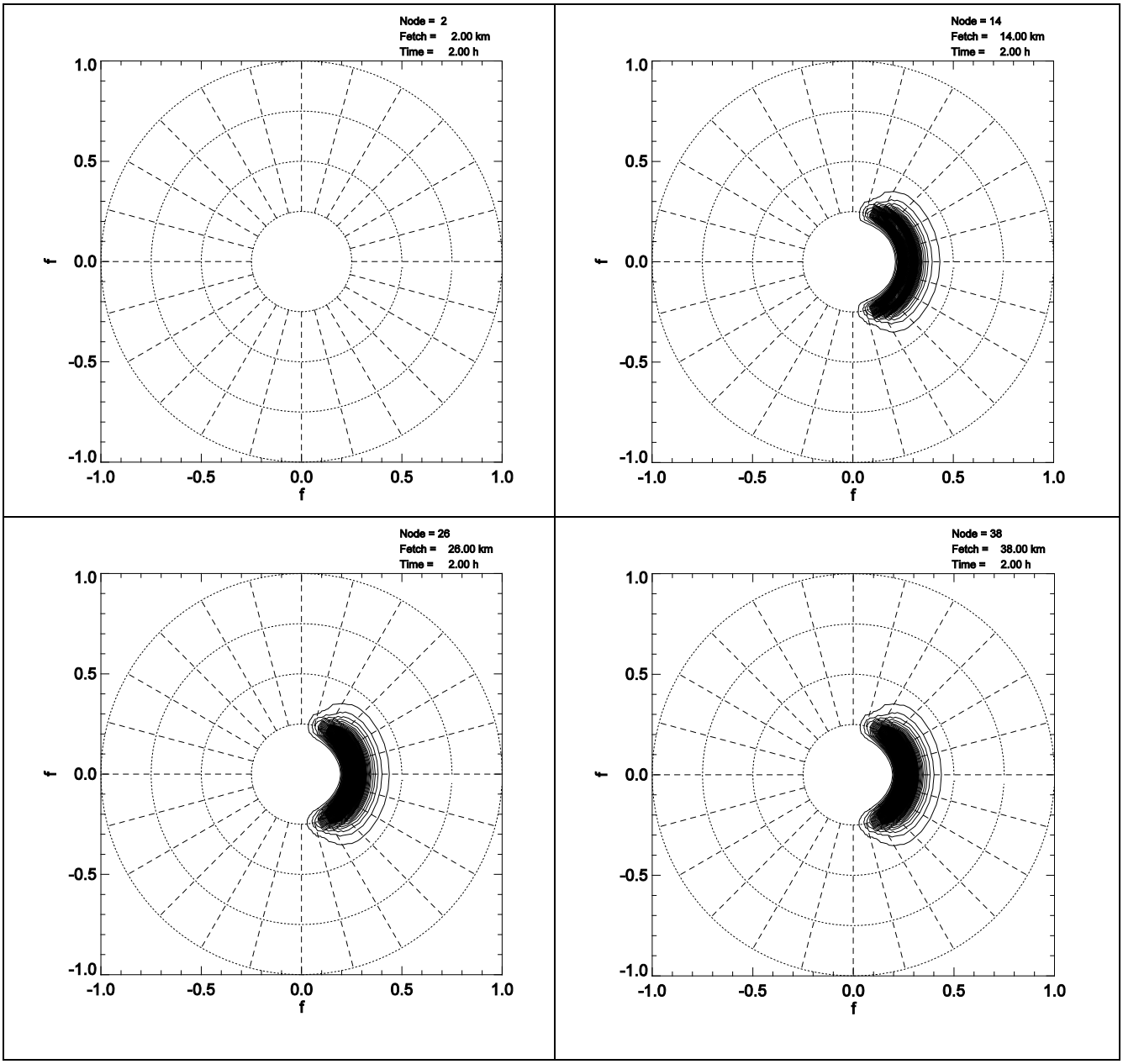

Fig.5b Spectral energy distribution as a function of frequency f and angle θ in polar coordinates at the fetch distances 2 km, 14 km, 26 km, 38 km for time 2hr.

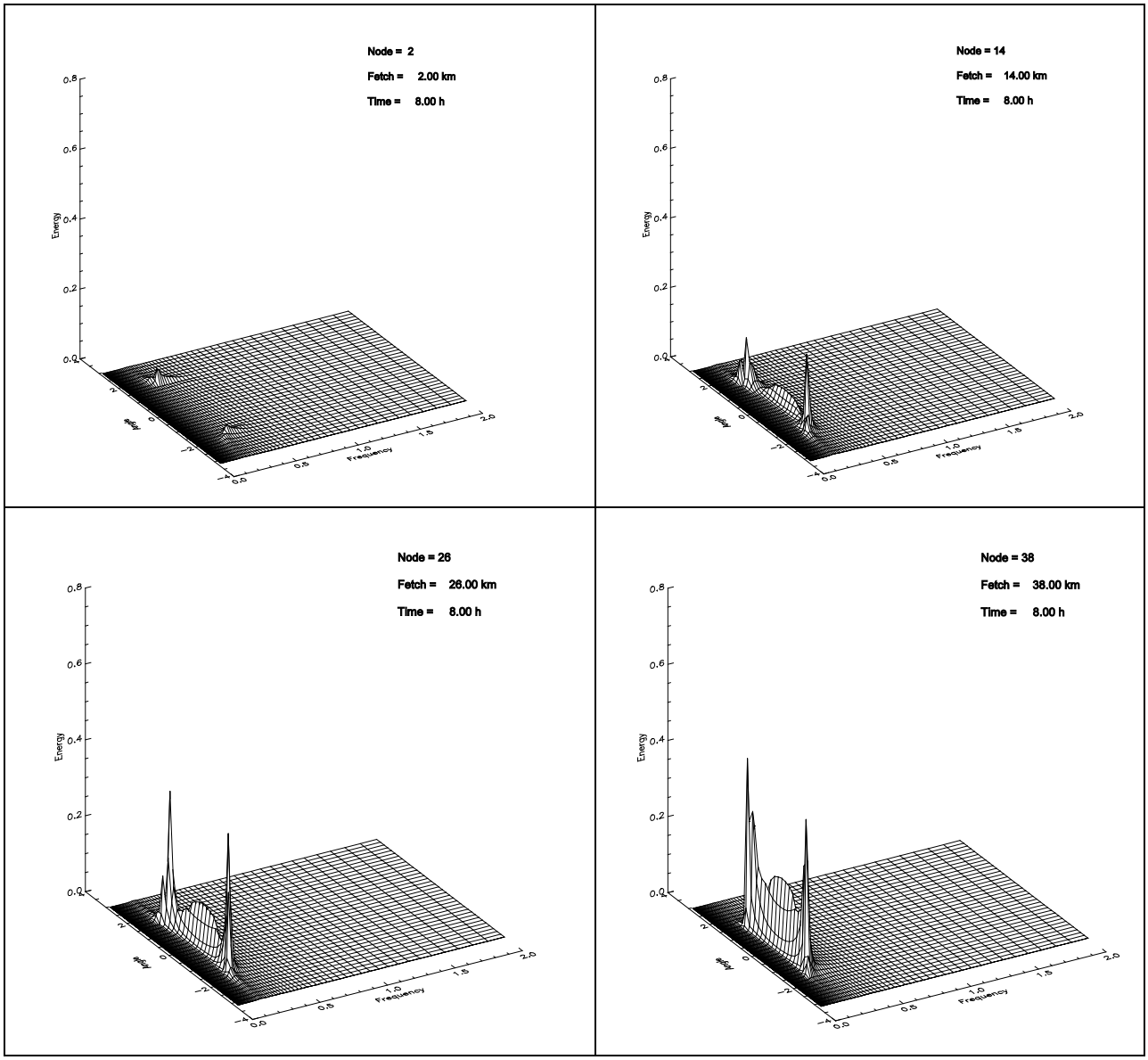

Fig.6a Spectral energy distribution as a function of frequency f and angle θ at the fetch distances 2 km, 14 km, 26 km, 38 km for time 8hr.

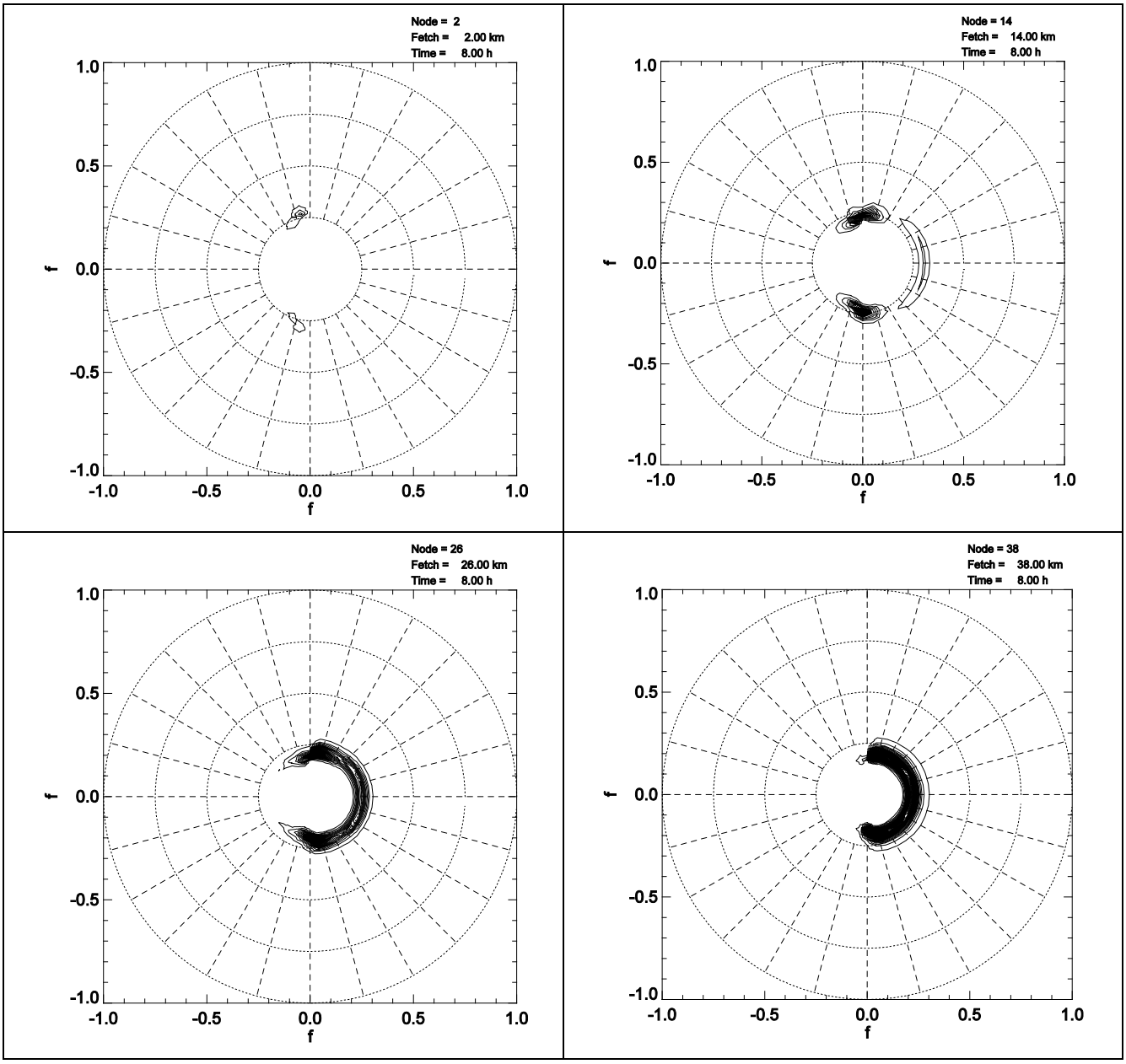

Fig.6b Spectral energy distribution as a function of frequency f and angle θ in polar coordinates at the fetch distances 2 km, 14 km, 26 km, 38 km for time 8hr.

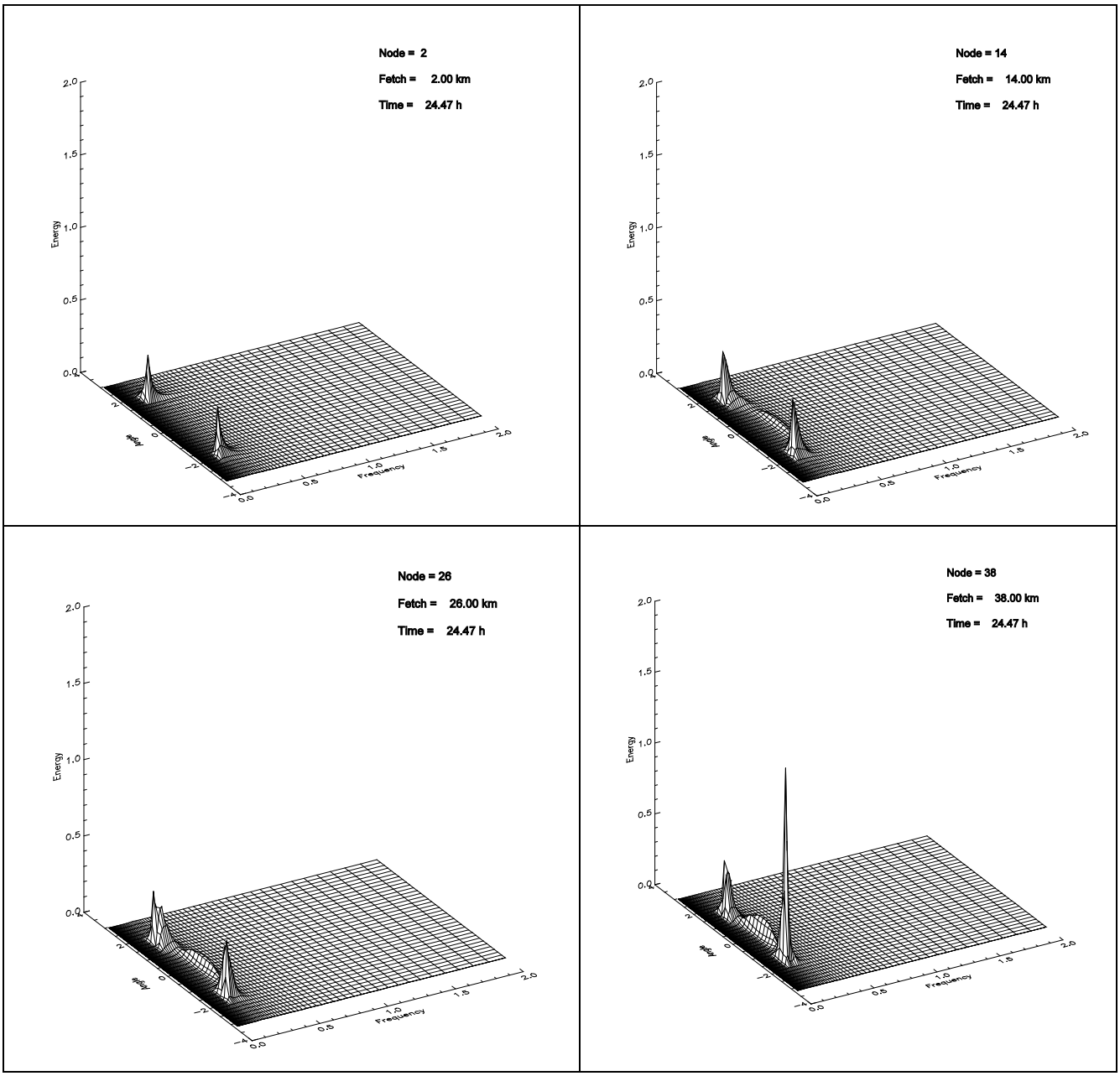

Fig.7a Spectral energy distribution as a function of frequency f and angle θ at the fetch distances 2 km, 14 km, 26 km, 38 km for time 24.47 hr.

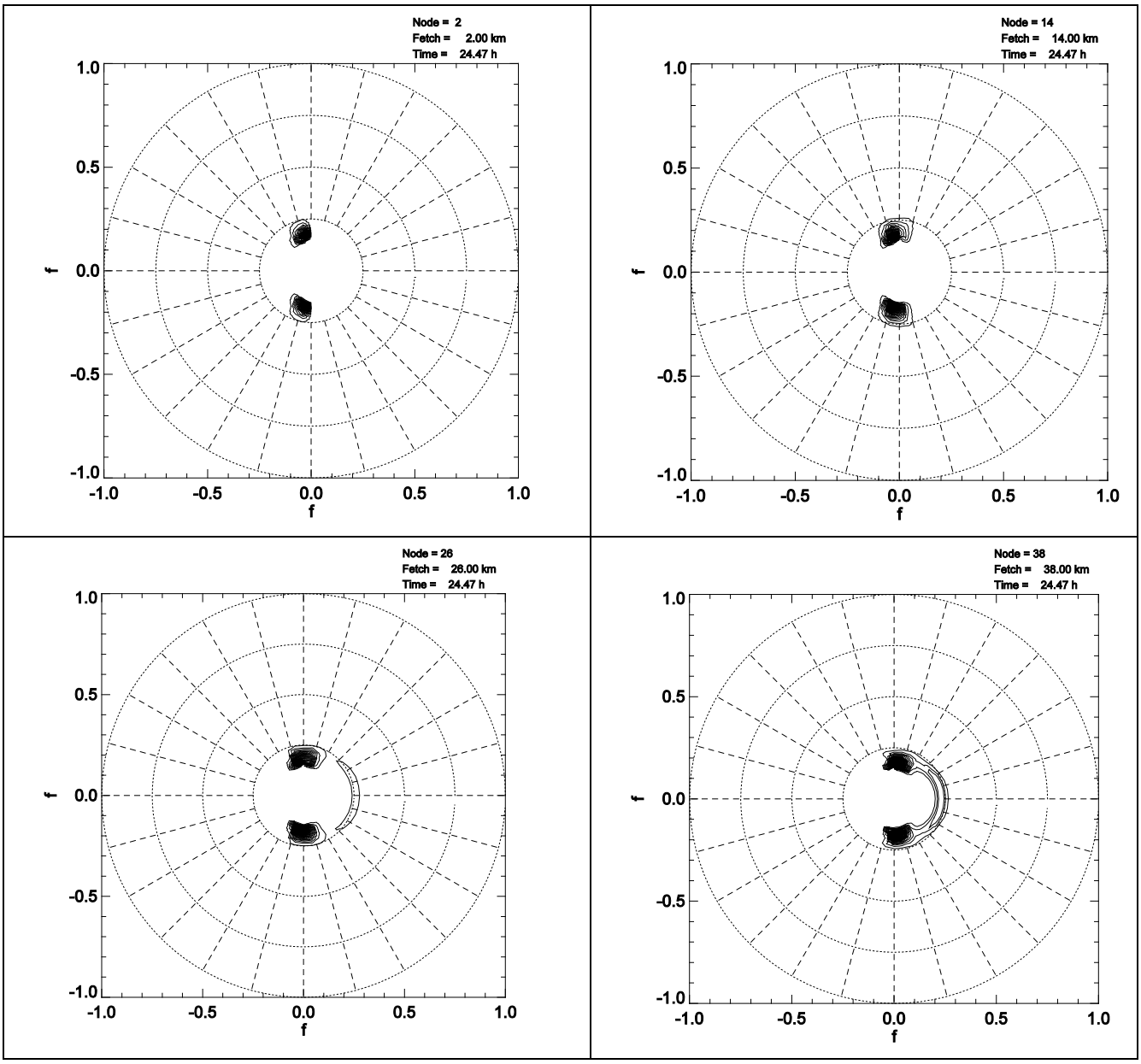

Fig.7b Spectral energy distribution as a function of frequency f and angle θ in polar coordinates at the fetch distances 2 km, 14 km, 26 km, 38 km for time 24.47 hr.

Research has been presented in **[P1], [P2].**

2. Physical model of sea wave period from altimeter data

We use the asymptotic theory of wind wave growth proposed in **[R6]** that predicts the Kolmogorov - like relationship between instant total wave energy $\boldsymbol{E}$ and total net wave forcing $\boldsymbol{S}$ (wave input minus dissipation). The latter can be associated with the observed rate of wave energy $\boldsymbol{dE/dt}$. Inversion of the so-called weakly turbulent law of wind-wave growth (see ***Eq. (1.9)*** in **[R6]**) gives a simple formula for period of spectral peak $\boldsymbol{T_p}$ as a function of significant wave height $\boldsymbol{H_s}$ and its gradient. The

relationship can be used for processing altimeter data assuming the wave field to be stationary and spatially inhomogeneous. It is consistent with satellite measurements setup and is written as follows

$$T_p=2^{1/5}\alpha_{ss}^{-3/10}(H_s/g)^{1/2}\times(\partial H_s/\partial s)^{-1/10} \quad (6)$$

Self-similarity parameter in ***Eq.(6)*** is set constant α_{ss}=0.67 as found in recent simulations of wind wave growth **[R7].** Wave height derivative along the wave propagation (group velocity) $\partial H_s/\partial s$ enters ***Eq.(6)*** in very low power *1/10* that reduces dramatically the effect of the unknown wave direction relative to the satellite track where the derivative can be estimated.

In contrast to all the models of wave periods mentioned above, ***Eq.(6)*** does not contain any empirical coefficients and, thus, does not require calibration. Additionally, it does not operate with backscatter coefficient σ_0, which characterizes sea surface roughness in gravity-capillary range and cannot be related to dominant waves straightforwardly.

The proposed method relies upon weakly turbulent mechanisms when instant sea state is determined by external flux to/from waves. The instant state and its apparent perturbation rate recorded by spatial derivative $\partial H_s/\partial s$ allow one to estimate wave period in certain range of scales. These scales should be sufficiently long as compared to the relaxation scales of weakly nonlinear surface waves and relatively short as compared to typical scales of variability of the wave field. Typical distance between two consecutive counts of satellite altimeter 5-7 kilometers (1 second) likely satisfies these simple criteria for sea waves and allows ***Eq.(6)*** to capture the weakly turbulent mechanism of wind-wave growth.

The new algorithm has been tested for the data collection of the ESA initiative Globwave (*http://www.globwave.org*). Different empirical models have been compared both for along-track records and in terms of statistical distributions of wave characteristics for particular ocean regions.

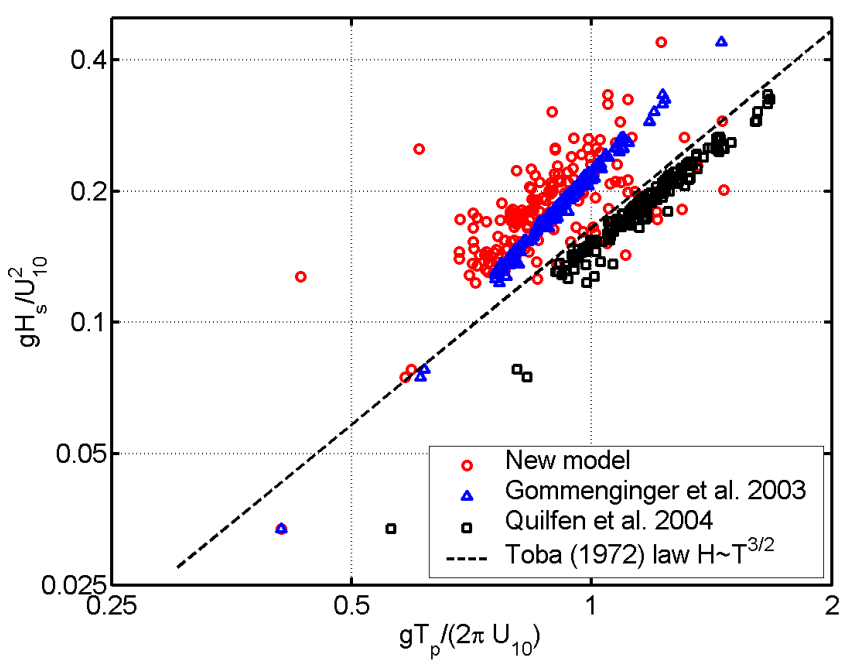

Fig. 8 Dependencies of non-dimensional wave height on non-dimensional wave period (wave age) calculated by different methods (see legend) for 800 km track of JASON-2 in the Caspian Sea, June 2, 2012.

Fig.8 presents an example of along-track evolution of non-dimensional wave height and period (wave age) calculated within different approaches **[R8], [R9].** The new model shows good agreement with previously proposed empirical dependencies. Relatively high dispersion of the new method (red points) can be partially explained by intentionally coarse data processing when neither smoothing nor interpolation of data has been used. At the same time, strong collapsing of results of calculations with **[R8], [R9]** in ***Fig.8*** looks suspicious enough: in situ experiments do show rather high dispersion relatively to "reference" growth curves like one of **[R10].** As our study shows, the "impoverishing" wave dynamics within the empirical parameterizations of wave period is well pronounced both for along-track cases like one presented above and in terms of statistical distributions for subsets of the Globwave data collection.

This study presents the very first results of the new model for wave periods from satellite altimeter data. The model is free of any empirical and tuning parameters, therefore, is independent on features of particular altimeter devices (if properly calibrated in wave height H_s) and regional peculiarities (say, extreme salinity in some inland basins).

Agreement with previously proposed approaches points to the validity of the asymptotic weakly turbulent law the new method is based on. While having very few in situ evidences of validity of the weakly turbulence theory for the wind-driven sea for the last 50 years, one has billions satellite altimeter records that are consistent with conclusions of this theory.

Results are published and presented in **[P3]-[P7].**

3. Prove of non-integrability of 1-D Zakharov equation and generalization of compact equation for almost 1-D waves

We studied amplitudes of six-wave interactions for compact 1-D Zakharov equation, Hamiltonian of which is:

$$H = \int b^* \hat{\omega}_k b dx + \frac{1}{2}\int |b'|^2 \left[\frac{i}{2}(bb'^* - b^* b') - \hat{k}\,|b|^2 \right] dx.$$

where $b' = \dfrac{\partial b}{\partial x}$, $\omega_k = \sqrt{gk}$ and $\hat{k}$ - modulus k operator.

It was found that six-wave amplitude (consisted of two four-wave amplitudes) is not canceled for this equation on the resonant manifold. Thus, it was proven that 1-D Zakharov equation is not integrable.

Also we have presented the results of numerical experiments on long time evolution and collisions of breathers (which correspond to envelope solitons in the NLSE approximation) at the surface of deep ideal fluid. The collisions happen to be nonelastic. In the numerical experiment "nonelasticity" can be observed only after many acts of interactions (collisions). This supports "deep water nonintegrability" numerically. One can see small radiation after 100 collisions of two breathers (solitions) on ***Fig. 9***:

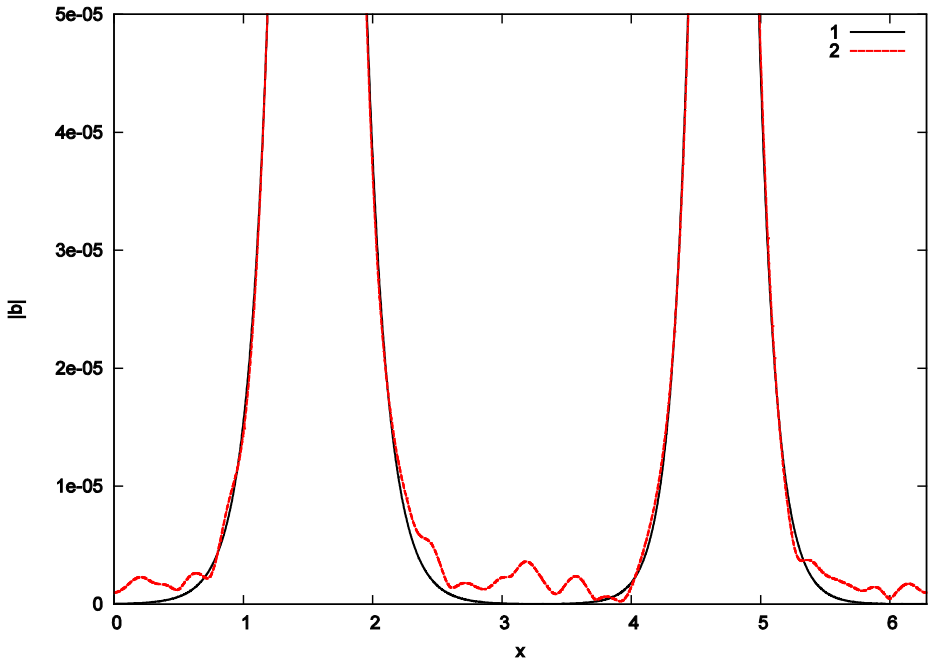

Fig.9 Appearance of small radiation (red line) as a result of 100 collisions of two breathers (black line)

We have derived generalization of compact equation for almost 1-D water waves, slightly modulated in transverse direction with the Hamiltonian as following:

$$H = \int b^* \hat{\omega}_{k_x,k_y} b dxdy + \frac{1}{2}\int |b'_x|^2 \left[\frac{i}{2}(bb'^*_x - b^* b'_x) - \hat{K}_x |b|^2 \right] dxdy.$$

Preliminary numerical experiments on freak-wave formation at the surface of 3D fluids were performed in the framework of this model. Typical picture of the surface with a freak wave is shown below on ***Fig.10*** :

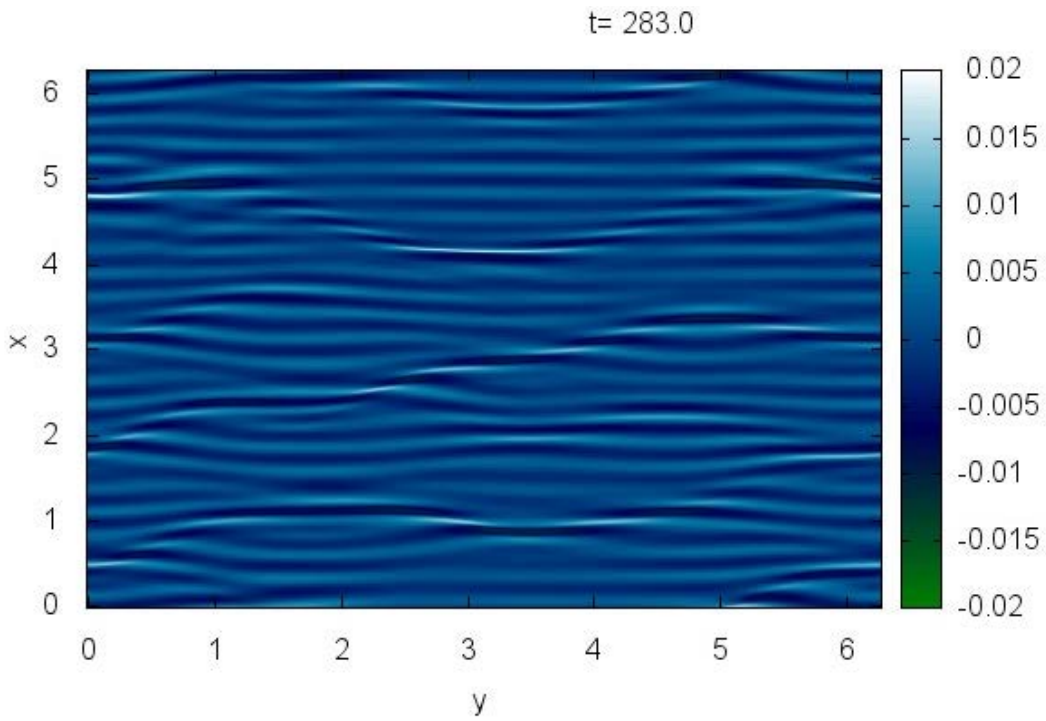

Fig.10 Typical picture of the surface with a freak waves as a result of numerical simulation of generalization of compact equation for almost 1-D water waves

Results are published and presented in **[P8]-[P15].**

4. Modulational instability and its implications for solitons, rogue waves and air-surface interactions

We studied the phenomenon of modulational instability. According to recent studies, the modulational instability seems to be a mechanism that is responsible for a number of phenomena that takes place in the ocean. In particular, experimental and numerical works have shown that the wave breaking mechanism and the formation of rogue waves may be caused by the modulational instability process.

In **[P16]** have performed direct numerical simulation of the Navier-Stokes equations for simulating a two-phase flow (water and air) to study the dynamics of the modulational instability of free surface waves and its contribution to the interaction between the ocean and atmosphere.

If the steepness of the initial wave exceeds a threshold value, we observed wave-breaking events and the formation of large-scale dipole structures in the air. Because of the multiple steepening and breaking of the waves under unstable wave packets, a train of dipoles is released in the atmosphere; those dipoles propagate at a height comparable with the wavelength. The amount of energy dissipated by the breaker in water and air is considered, and contrary to expectations, we have observed that the energy dissipation in air is greater than that in water. The possible implications for the wave modeling of aerosols and gases exchange between air and water are also discussed in the paper.

In **[P17]** the rogue wave solutions (rational multi-breathers) of the nonlinear Schrodinger equation (NLS) are tested in numerical simulations of weakly nonlinear and fully nonlinear hydrodynamic equations. A higher accuracy of wave propagation in space is reached using the modified NLS

equation, i.e. Dysthe equation. This numerical modeling allowed us to directly compare simulations with recent results of laboratory measurements **[R11].** In order to achieve even higher physical accuracy, we employed fully nonlinear simulations of potential Euler equations. These simulations provided us with basic characteristics of long time evolution of rational solutions of the NLS equation in the case of near-breaking conditions. The analytic NLS solutions are found to describe the actual wave dynamics of steep waves reasonably well.

In paper **[P18]** the problem of existence of stable nonlinear groups of gravity waves in deep water is considered by means of laboratory and numerical simulations with the focus on strongly nonlinear waves. Wave groups with steepness up to 0.30 are reproduced in laboratory experiments. We show that the groups remain stable and exhibit neither noticeable radiation nor structural transformation for more than 60 wavelengths or about 15-30 group lengths. These solitary wave patterns differ from the conventional envelope solitons, as only a few individual waves are contained in the group. Very good agreement is obtained between the laboratory results and numerical simulations of the potential Euler equations. The envelope soliton solution of the nonlinear Schrodinger equation is shown to be a reasonable first approximation for specifying the wave-maker driving signal. The short intense envelope solitons possess vertical asymmetry similar to regular Stokes waves with the same frequency and crest amplitude. Nonlinearity is found to have remarkably stronger effect on the speed of envelope solitons in comparison to the nonlinear correction to the Stokes wave velocity.

In paper **[P19]** we show experimentally that a stable wave propagating into a region characterized by an opposite current may become modulationally unstable. Experiments have been performed in two independent wave tank facilities; both of them are equipped with a wave-maker and a pump for generating a current propagating in the opposite direction with respect to the waves. The experimental results support a recent conjecture based on a current-modified nonlinear Schrodinger equation which establishes that rogue waves can be triggered by a non-homogeneous current characterized by a negative horizontal velocity gradient.

The paper **[P20]** is a review paper on rogue waves in different physical aspects ranging from oceanography to nonlinear optics.

In the paper **[P21]** we present the first observation of dark solitons on the surface of water. It takes the form of an amplitude drop of the carrier wave which does not change shape in propagation. The shape and width of the soliton depend on the water depth, carrier frequency, and the amplitude of the background wave. The experimental data taken in a water tank show an excellent agreement with the theory. These results may improve our understanding of the nonlinear dynamics of water waves at finite depths.

In paper **[P22]** we highlight an analogy between water waves and electromagnetic waves, i.e. the formation of a supercontinuum: starting from a very narrow band spectrum, after a few wave lengths, a very broad continuum spectrum (supercontinum) is observed with a consequent emission of solitons.

5. Approximate model for 1D deep water surface waves based on MMT equation

We studied analytically and numerically the Majda–McLaughlin–Tabak (MMT) model

$$i\frac{\partial \psi_k}{\partial t} = |k|^{\alpha}\psi_k + \lambda \int T_{kk_1k_2k_3}\psi^*_{k_1}\psi_{k_2}\psi_{k_3}\delta_{k+k_1+k_2+k_3}dk_1dk_2dk_3$$

$$T_{kk_1k_2k_3} = |k|^{\beta/4}|k_1|^{\beta/4}|k_2|^{\beta/4}|k_3|^{\beta/4}$$

adjusted for description of essentially nonlinear gravity waves on the surface of ideal deep water through specific choice of its parameters α = 1/2, β =3 and λ = 1.

The water surface can be reconstructed from complex function $\psi(x,t)$ through the following relation:

$$\eta(x,t) = \frac{1}{\sqrt{2}}\int e^{ikx}|k|^{1/4}\left(\psi_k + \psi^*_{-k}\right)dk \tag{7}$$

On the base of analytic study and numerical experiments, we observe existence of robust long-living objects in the form of quasi-stationary localized structures, which are the quasisolitons.

Quasisolitons of large amplitude turn into quasibreathers. Their amplitude and spectral shape oscillate in time (see ***Fig.11***).

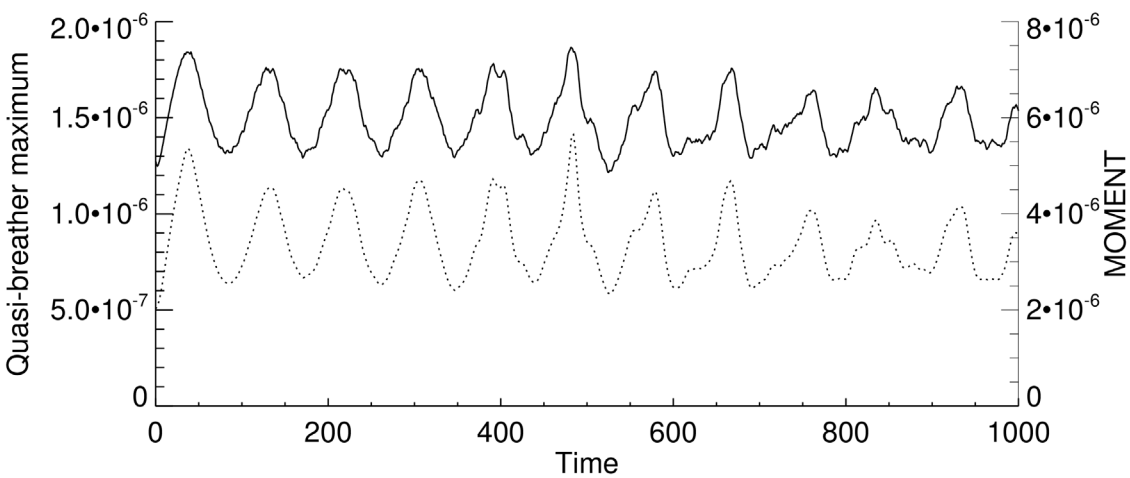

Fig.11 Dependence of the soliton maximum $\max(|\psi(x,t)|^2)$ ***taken over integration domain*** $[0,2\pi]$ ***(solid line, left axis) and the second moment*** $\int (k-k_0)^2|\psi_k|^2\,dk$ ***(dotted line, right axis), on time t.***

The average wave-number is defined as $k_0 = \dfrac{\int k|\psi_k|^2 dk}{\int |\psi_k|^2 dk}$

These oscillations at the time moment of reaching the quasibreather maximum are accompanied by formation of weak collapses, exhibiting their selves through power-like spectra, which can be compared with ‘‘white capping’’ of real ocean waves, see ***Fig.12.***

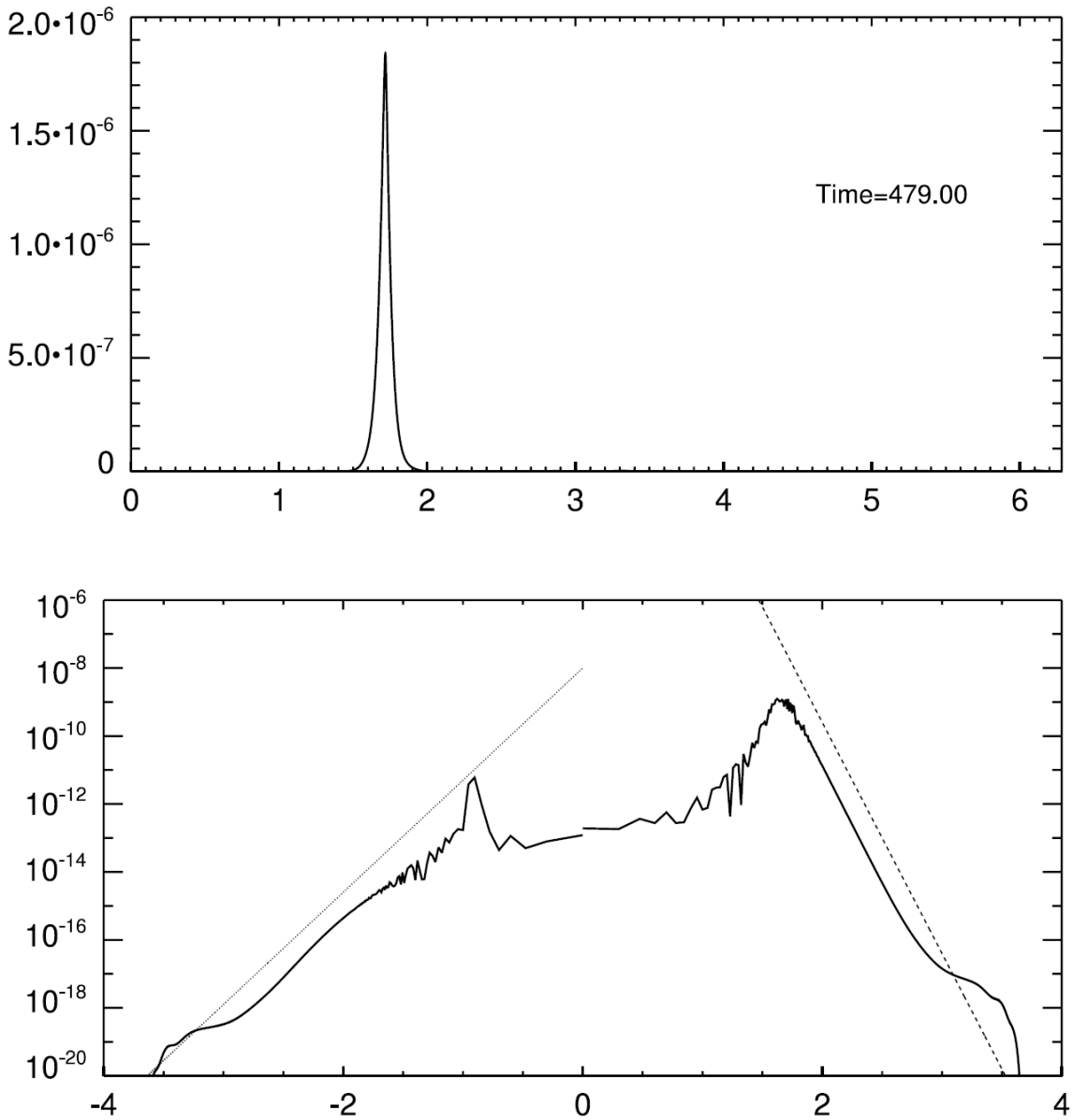

Fig.12 Real and Fourier space distributions of wave field. Top graph: $|\psi(x,t)|^2$ ***as a function of x for t=479.00. Bottom graph: Fourier spectrum*** $\log_{10}|\psi(x,t)|^2$ ***as a function of signed logarithm of wave number*** $sign(k)\log_{10}|k|$***. The left slope of the spectrum is approximated by function*** $\propto k^{-3.3}$ ***(dotted line); the right slope is approximated by function*** $\propto k^{-6.8}$ ***(dashed line).***

Fig.13 presents surface elevations ***Eq.(7)*** for the same time as ***Fig.12***. This picture looks qualitatively similar to experimentally observes "Three Sisters" killer wave on the ocean surface **[R12]** and the resent results of freakon simulation on the deep water surface **[R13].** These slope values have the meaning of the original Euler equations for deep waver surface gravity waves.

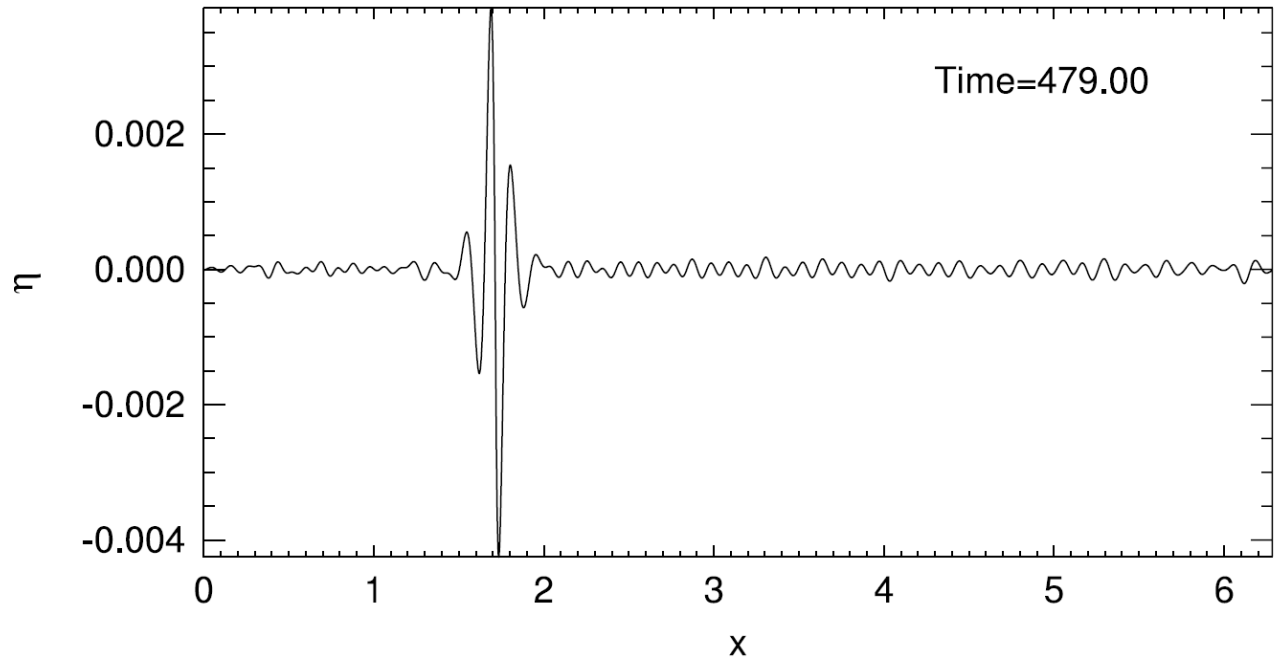

Fig.13 Surface elevations $\eta(x,t)$ as a function of real space coordinate x for time t=479.00, corresponding to Fig.12. The presented data are dimensionless and scale invariant due to this property of the corresponding equations. For the purposes of comparison with the experiment, one should multiply both horizontal and vertical axes by the same dimensional factor, corresponding to particular experimental realization.

The research has been published in **[P23].**

REFERENCES

[R1] V. E. Zakharov, D. Resio, A. Pushkarev, New wind input term consistent with experimental, theoretical and numerical considerations, **arXiv:1212.1069 [physics.ao-ph]**

[R2] Resio D., Long C., Equilibrium-range constant in wind-generated spectra, Journal of Geophysical Research, v.109, CO1018, 2004

[R3] Long, C.E, and D. Resio, Wind wave spectral observations in Currituck Sound, North Carolina Journal of Geophysical Research, v. 112, CO5001, 2007

[R4] Second year NOPP ONR report, Nonlinearity Role in Long-Term Interaction of the Ocean Gravity Waves, 2012

[R5] Zakharov, V.E. Nonlinear Processes in Geophysics, 12, 1011–1020, 2005

[R6] Badulin, S. I., A. V. Babanin, D. Resio, and V. Zakharov, Weakly turbulent laws of wind-wave growth, *J. Fluid Mech.*, *591*, 339–378, 2007.

[R7] Gagnaire-Renou, E., M. Benoit, and S. I. Badulin, On weakly turbulent scaling of wind sea in simulations of fetch-limited growth, *J. Fluid Mech.*, *669*, 178–213, 2011.

[R8] Gommenginger, C. P., M. A. Srokosz, P. G. Challenor, and P. D. Cotton, Measuring ocean wave period with satellite altimeters: A simple empirical model, *Geophys. Res.Lett.*, *30* (22), 2150, doi:10.1029/ 2003GL017743, 2003.

[R9] Quilfen, Y., B. Chapron, and M. Serre, Calibration/validation of an altimeter wave period model and application to TOPEX/Poseidon and Jason-1 altimeters, *Marine Geodesy*, *27*, 535–549, 2004.

[R10] Toba, Y., Local balance in the air-sea boundary processes. Part I. On the growth process of wind waves, *J. Oceanogr. Soc. Japan*, *28*, 109–121, 1972.

[R11] A. Chabchoub, N. Akhmediev & N. Hoffmann, 'Experimental study of spatiotemporally localized surface gravity water waves', Physical Review E-Statistical, Nonlinear and Soft Matter Physics, vol. 86, no. 1, pp. 016311 (2012)

[R12] C.Kharif, E.Pelinovsky, A.Slunyaev, Rogue Waves in the Ocean, Springer, ISBN 3540884181, 2009

[R13] V.E.Zakharov, A.I.Dyachenko, About shape of giant breather, Eur.J.Mech.B-Fluids, 29 (2010), 127-131

PUBLICATIONS

[P1] V.E. Zakharov, A.N.Pushkarev, Nonlinear generation of surface waves against the wind in a limited fetch growth model . 20th meeting WISE. April 21-25, 2013, College Park, Maryland, USA **[oral talk]**

[P2] A.N.Pushkarev, V.E. Zakharov Nonlinear generation of surface waves against the wind in a limited fetch growth model. XXV IUPAP Conference on Computational Physics, Moscow, Russia, August 20-24, **[oral talk]**

[P3] S. I. Badulin, A physical model of sea wave period from altimeter data. **Submitted** to Journal of Geophysical Research August 6, 2013.

[P4] S.I. Badulin, V.G. Grigorieva, V.E. Zakharov, On relaxation due to nonlinear transfer and physical model of wave periods from satellite altimeters. 20th meeting WISE. April 21-25, 2013, College Park, Maryland, USA **[oral talk]**

[P5] Sergei I. Badulin, Vladimir E. Zakharov, Andrei N. Pushkarev, Simulation of wind wave growth with reference source functions, Geophysical Research Abstracts, Vol. 15, EGU2013-5284-1, 2013, EGU General Assembly 2013 **[published]**

[P6] S. I. Badulin and V. G. Grigorieva, Weak turbulence theory as a ground for measurements of wind wave periods by satellite methods, International Conference FRONTIERS OF NONLINEAR PHYSICS Nizhny Novgorod, Russia, July 28 - August 2, 2013, **[published]**

[P7] S.I. Badulin, V.G. Grigorieva, A Physical Model of Sea Wave Period from Altimeter Data, ESA Living Planet Symposium, 9 - 13 September, 2013, Edinburgh, United Kingdom **[published]**

[P8] A.I. Dyachenko, D.I. Kachulin and V.E. Zakharov, "On the Nonintegrability of the Free Surface Hydrodynamics", JETP Letters, V. 98(1), (2013) хжф. 43-47 **[published]**

[P9] Dyachenko A.I., Kachulin D.I. and Zakharov V.E., "Collisions of two breathers at the surface of deep water", Natural Hazards and Earth System Sciences, Special Issue: Extreme seas and ship operations, (2013) [**publlished**]

[P10] Dyachenko A.I. Zakharov V.E., Shamin R.V. and Badulin S.I., "Freak waves and problems of their study", In the book "Mirovoi Okean" V.1., Ed. L.I. Lobkovskii, p. 576-592, 2013 **[published]**

[P11] IUTAM Symposium 2013: Nonlinear interfacial wave phenomena from the micro to the macro-scale, Limassol, Cyprus, April 14-18, 2013, A.I. Dyachenko, V.E. Zakharov, D.I. Kachulin, "Compact dynamical equation for 2D water waves" **[oral talk]**

[P12] International Conference "Landau Days-2013", Chernogolovka, Russia, June 24-26, 2013, A.I. Dyachenko, D.I. Kachulin, V.E. Zakharov, "Compact equation for 2D water waves" **[oral talk]**

[P13] V International Conference "Frontiers of nonlinear physics", Nizhny Novgorod, Russia, July 28-August 2, D.I. Kachulin, A.I. Dyachenko, V.E. Zakharov, "Analysis of integrability of the free surfaces hydrodynamics equation for deep water" **[oral talk]**

[P14] International Conference "FLUXES AND STRUCTURES IN FLUIDS", St. Petersburg, June 25-28, 2013, Kachulin D.I., Dyachenko A.I., Zakharov V.E. "Nonintegrability of Hydrodynamics Equation for Deep Water Gravity Waves" **[oral talk]**

[P15] XXV IUPAP Conference on Computational Physics, Moscow, Russia, August 20-24, A.I. Dyachenko, D.I. Kachulin, V.E. Zakharov, "Freak waves at the surface of deep water" **[oral talk]**

[P16] Iafrati, A; Babanin, A; Onorato, M Physical Review Letters,Volume: 110 Issue: 18 Pages: 184504 **[published]**

[P17] Slunyaev, A.; Pelinovsky, E.; Sergeeva, A.; Chabchoub, A; Hoffmann, N; Onorato, M.; Akhmediev, N PHYSICAL REVIEW E Volume: 88 Issue: 1 Article 012909 DOI: 10.1103/PhysRevE.88.01290 **[published]**

[P18] Slunyaev, A.; Clauss, G. F.; Klein, M.; Onorato, M. PHYSICS OF FLUIDS Volume: 25 Issue: 6 Article Number: 067105 DOI: 10.1063/1.4811493 **[published]**

[P19] A.Toffoli, T. Waseda, H. Houtani,T. Kinoshita, K. Collins, D. Proment, and M. Onorato PHYSICAL REVIEW E (Rapid Comminication) 87, 051201(R) (2013) 1539 3755/2013/87(5)/051201(4) **[published]**

[P20] M.Onorato, S. Residori, U. Bortolozzo, A. Montina, F.T. Arecchi Physics Reports 528 (2013) 47/89 http://dx.doi.org/10.1016/j.physrep.2013.03.001 **[published]**

[P21] A. Chabchoub, O. Kimmoun, H. Branger, N. Hoffmann, D. Proment, M. Onorato and N. Akhmediev PHYSICAL REVIEW LETTERS Volume: 110 Issue: 12 Article Number: 124101 DOI: 10.1103/PhysRevLett.110.124101 **[published]**

[P22] Chabchoub, A; Hoffmann, N; Onorato, M; Genty, G; Dudley, J M; Akhmediev, N Physical Review Letters Volume: 111 Issue: 5 Pages: 054104 (Epub 2013 Aug 02) **[published]**

[P23] A.Pushkarev, V.E.Zakharov, Quasibreathers in the MMT model, Physica D, 248, 55-61, 2013 **[published]**